NANO LETTERS

Letter

pubs.acs.org/NanoLett

Scaled Synthesis of Boron Nitride Nanotubes, Nanoribbons, and Nanococoons Using Direct Feedstock Injection into an Extended-Pressure, Inductively-Coupled Thermal Plasma

Aidin Fathalizadeh,[†,‡] Thang Pham,[†,‡,§] William Mickelson,[†,∥] and Alex Zettl*[,†,‡,∥,⊥]

[†]Department of Physics, [§]Department of Materials Science and Engineering, and [∥]Center of Integrated Nanomechanical Systems, University of California at Berkeley, Berkeley, California 94720, United States

[‡]Materials Sciences Division, Lawrence Berkeley National Laboratory, Berkeley, California 94720, United States

[⊥]Kavli Energy NanoSciences Institute at the University of California, Berkeley and the Lawrence Berkeley National Laboratory, Berkeley, California 94720, United States

ABSTRACT: A variable pressure (up to 10 atm) powder/gas/liquid injection inductively coupled plasma system has been developed and used to produce high-quality boron nitride nanotubes (BNNTs) at continuous production rates of 35 g/h. Under suitable conditions, collapsed BN nanotubes (i.e., nanoribbons), and closed shell BN capsules (i.e., nanococoons) are also obtained. The process is adaptable to a large variety of feedstock materials.

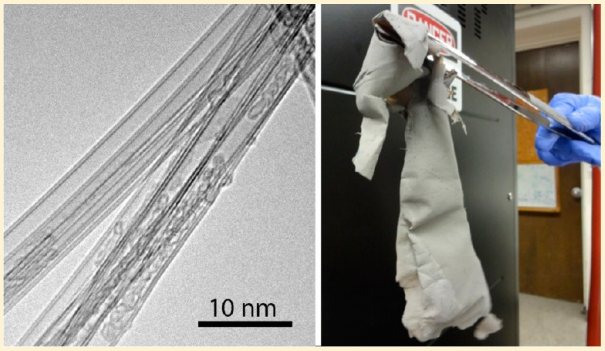

KEYWORDS: *Boron nitride nanotubes, scalable nanotube synthesis, inductively coupled plasma, hyperbaric plasma*

Boron nitride nanotubes (BNNTs), first synthesized in 1995 by Zettl and collaborators,[1] are wide-bandgap structural analogues[2] to carbon nanotubes.[3] Importantly, the special chemical, optical, thermal, and radiation-absorption properties of BNNTs make them far superior to their carbon counterparts for many applications.[4] Theoretical[5] and experimental[6,7] studies demonstrate that the electronic energy bandgap is ~5 eV independent of tube diameter and chirality but can be tuned by the application of transverse electric fields.[6] A host of other BNNT properties have been considered, including tunable thermal conductivity,[8] piezoelectricity,[9] biocompatibility,[10] hosts for silocrystal structures,[11] electron field emission,[12] water purification,[13] and reinforcements for structural composites,[14,15] to name just a few.

An unfortunate constraint that has severely limited the scientific study and industrial application of BNNTs and related BN-based nanostructures, such as BN nanoribbons (BNNRs) and BN nanococoons (BNNCs), is the general lack of availability of the synthesized materials. The original arc-plasma synthesis method of BNNTs has seen some refinements,[16] but generally it is not readily scalable. Other synthesis methods have been advanced, including laser vaporization,[17] chemical vapor deposition,[18,19] plasma torch,[20] ball milling and annealing,[21] and templated conversion.[22,23]

A noteworthy advance in BNNT synthesis occurred in 2009 using a laser ablation technique to create small-wall-number, highly crystalline, and high aspect ratio pure BNNTs.[24] This catalyst-free synthesis technique utilizes a kilowatt-power laser to ablate a boron target in a high-pressure nitrogen atmosphere. The boron vapor created by the laser is condensed on a filament after which it reacts with the nitrogen gas to create BNNTs. Unfortunately, the laser-vaporization method of Smith et al.[24] suffers from low energy efficiency as well as limited throughput (approximately 100 mg/h). Nevertheless, it suggests that, given the right local high input energy flux and quenching dynamics, scaled production of BNNTs and related BN nanoparticles should be achievable. Furthermore, it elucidates two key aspects of high purity BNNT production from boron precursors: (1) high-pressure nitrogen environments are effective in driving the reaction from B and N_2 to BN, and (2) controllable introduction of liquid boron droplets can precipitate BNNTs without a catalyst.

High-power, low-pressure inductively coupled plasma systems have been successfully used in the scaled synthesis of carbon nanotubes.[25] Here, we demonstrate the successful operation of a high-throughput, scalable BN nanostructures synthesis process whereby precursor materials are directly and continuously injected into a high-temperature, extended-pressure inductively-coupled plasma system (EPIC). The EPIC synthesis system, an implementation of a design

Received: June 18, 2014
Revised: July 8, 2014
Published: July 8, 2014

   dx.doi.org/10.1021/nl5022915 | *Nano Lett.* 2014, 14, 4881−4886

previously proposed by one of the authors,[26] is remarkably versatile in terms of synthesis parameters and allows for the injection of fluids (gases or liquids) and solids (powders) directly into the variable-power plasma plume. In addition, the high-pressure capability of the plasma (up to 10 atm) allows for dramatic shifts in chemical reaction tipping points. The system can be operated in a near-continuous fashion and thus far has achieved a record output of over 35 g/h for pure, small diameter, few wall, highly crystalline BNNTs.

Inductively coupled thermal plasma systems typically operate at reduced pressure (1 atm and below), and no commercial system exists that is capable of operating within our desired parameter range (including high pressure, pure nitrogen operation). Therefore, we have designed and custom-built a suitable EPIC synthesis system from the ground up. Details of the design and construction of the system will be presented elsewhere, but the key features are described below.

Figure 1 shows a schematic of the EPIC system. A plasma-generating torch, driven by a 60 kW, 7 MHz power supply and suitable matching network, is mounted atop a 15 cm inner diameter, 112 cm long synthesis chamber. Several access ports in the torch and synthesis chamber provide for materials injection/extraction and diagnostics or for introducing quench-enhancers (such as wires or meshes). For example, the plasma gas (nitrogen) can be introduced at port A, and boron feedstock (e.g., pure boron powder) can be injected directly into the plasma plume via port B. Other modes of operation are possible, such as coinjection of the plasma gas and boron feedstock through port A, or introducing the plasma gas through port C where the gas first swirls upward along the inner wall of the torch body and then back down the center. For powder injection, a commercial powder feeder (Powder Feed Dynamics, Mark XV) is employed. The entire system (power supply, torch, and synthesis chamber) is water-cooled to allow for continuous operation and to ensure suitable thermal quench gradients within the synthesis chamber. Synthesized material can be collected manually from the opened synthesis chamber, or more practically, via an in situ pressure-purge extraction cycle which affords near-continuous (rather than batch) operation.

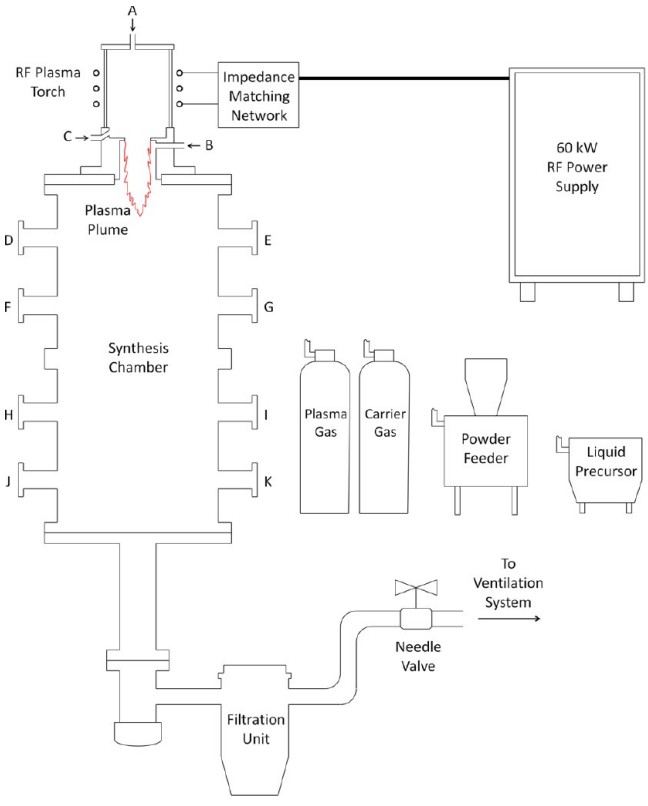

Figure 1. Schematic of a custom-built extended pressure inductively coupled (EPIC) thermal plasma system for the scaled synthesis of BNNTs and related materials. Ports A, B, and C are for injection of plasma gas and/or feedstock near the plasma plume, while ports D−K are for diagnostics (such as optical monitoring of the reaction) and/or for insertion of quench modifiers or pressure-assisted purging of synthesized material. Powder feedstock is sourced from a commercial powder feeder using carrier gas, while liquids/gases are direct injection. The entire system, including power supply, torch, and synthesis chamber, is water-cooled (cooling details not shown). For a typical run described in this report, the plasma gas is pure N_2 injected into port A, and the boron feedstock is pure boron powder or hBN powder injected via powder feeder and pure N_2 carrier gas into port B.

The power density and volume of the plasma plume, which have direct bearing on the temperature, residence time of precursor materials, and quench rates in the reaction zone, can be modified at any given pressure by varying the input power and gas flow rates. Quench rates are further tuned by varying the cooling water flow rate to the synthesis chamber or by lining the interior wall of the synthesis chamber with thermal blankets (in some runs carbon felt of 1.3 cm thickness was used with good results).

Although we have explored only a small fraction of the large parameter space afforded by the EPIC system, we find that with this approach the synthesis of BNNTs is remarkably effective and robust, producing high quality materials at record production rates of 35 g/h. In the discussion below, we limit ourselves to synthesis runs in which no special quench wires or screens are used, the plasma gas is pure nitrogen injected via port A, and the boron feedstock is either hexagonal BN (hBN) powder (Alfa Aesar, −325 mesh) or amorphous boron powder (Alfa Aesar, −325 mesh) delivered by nitrogen carrier gas. In no case is a catalyst used. Both types of boron feedstock successfully produce BNNTs (and with suitable parameter adjustment other BN nanomaterials, see below), but a higher conversion rate is achieved with amorphous boron powder. Nitrogen as the carrier gas (2−5 L/min) is used to propel the powder radially into the plasma plume via port B near the torch nozzle at pressures varying from 14.7−75 psia (psi absolute), with boron injection rates between 100 and 1700 mg/min. Nitrogen flowing at 50 L/min serves as the plasma gas with plasma power maintained between 40 and 50 kW. Exploratory runs have a typical duration of 10 min to an hour.

Under the above conditions, the EPIC system immediately generates a fibrous, light-colored, cotton-candy web-like material, which soon occupies the entire cross-sectional area of the synthesis chamber, as shown in Figure 2a. The material initially accumulates in the upper half of the chamber (near the torch hot zone), and as the run is continued, the synthesis chamber gets successively packed, filling a volume of 10 L (half the total chamber volume) in approximately 30 min. In conjunction with fibrils packing the interior volume of the synthesis chamber, the chamber walls typically also become coated in a similarly light colored material, which can be easily peeled off as a continuous felt-like film (Figure 2b). Often the fibril and felt materials have an overall light grayish color, which

dx.doi.org/10.1021/nl5022915 | Nano Lett. 2014, 14, 4881−4886

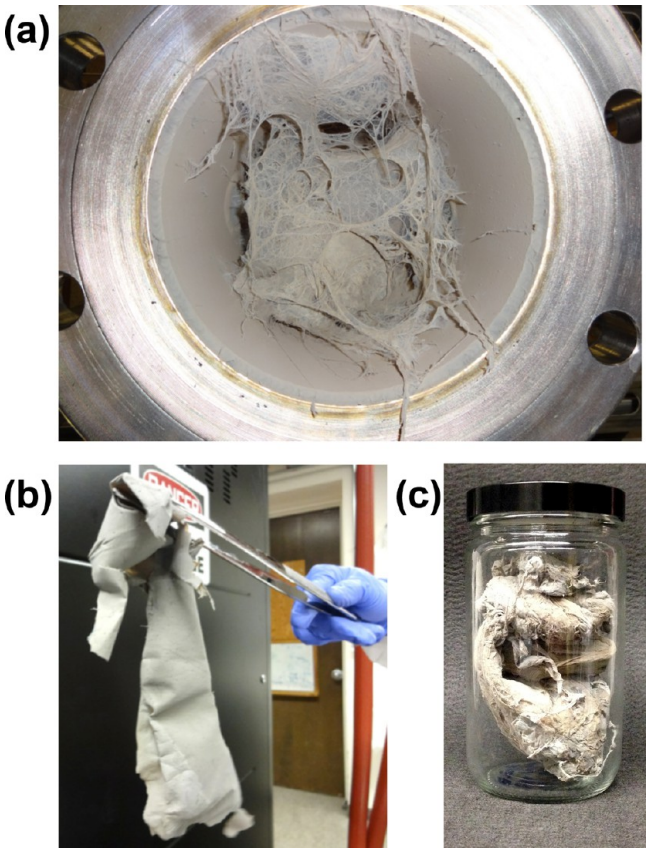

Figure 2. Photographs of BNNT material produced via the EPIC method. (a) As-synthesized BNNT fibril material accumulated within 15 cm diameter synthesis chamber, as seen from below. After a few minutes of run time, the fibril mass completely fills the cross-sectional upper area of the chamber. As the reaction proceeds, the synthesized BNNTs fill more and more of the chamber volume. (b) BNNT felt-like sheet peeled intact from the walls of the reaction chamber. (c) Compressed BNNT fibril material (from a 15 min synthesis run) fills a one-liter glass jar. For a, b, and c the material is composed largely of double-wall BNNTs. Synthesis conditions: amorphous boron @ 246 mg/min; carrier gas N_2 @ 2.5 L/min; plasma gas N_2 @ 50 L/min; 40 kW plasma @ 30 psia.

on closer inspection reveals itself as pure-white cottony patches dispersed among grayish material.

We have characterized both the fibril cotton-candy-like and felt-like sheet material and find that, over a broad range of synthesis conditions, both are composed predominantly of pure BNNTs (up to 80% yield) with wall number ranging from two to six, with the most common being double−wall tubes of outer diameter ∼4 nm similar to those observed using other BNNT synthesis techniques.[16] The grayish color originates from dark specks of unreacted boron (typically 20% of product) not incorporated into the pure-white (or rather transparent) tubes and is easily removed by treatment in a nitric acid solution.[16]

The nanoscopic morphology and purity of the BNNT-containing material are elucidated using scanning electron microscopy (SEM) (FEI Sirion XL30) with energy dispersive X-ray analysis (EDAX) capability and transmission electron microscopy (TEM) (JEOL JEM 2010 operating at 80 kV). Element-sensitive electron energy loss spectroscopy (EELS) is performed using a Phillips CM-200 and a FEI Tecnai G2 TEM both operated at 200 kV. Raman spectra are collected on a Renishaw inVia spectrometer using a 514 nm excitation laser.

Figure 3 shows characteristic SEM images of the fibril-like material removed from the center of the synthesis chamber.

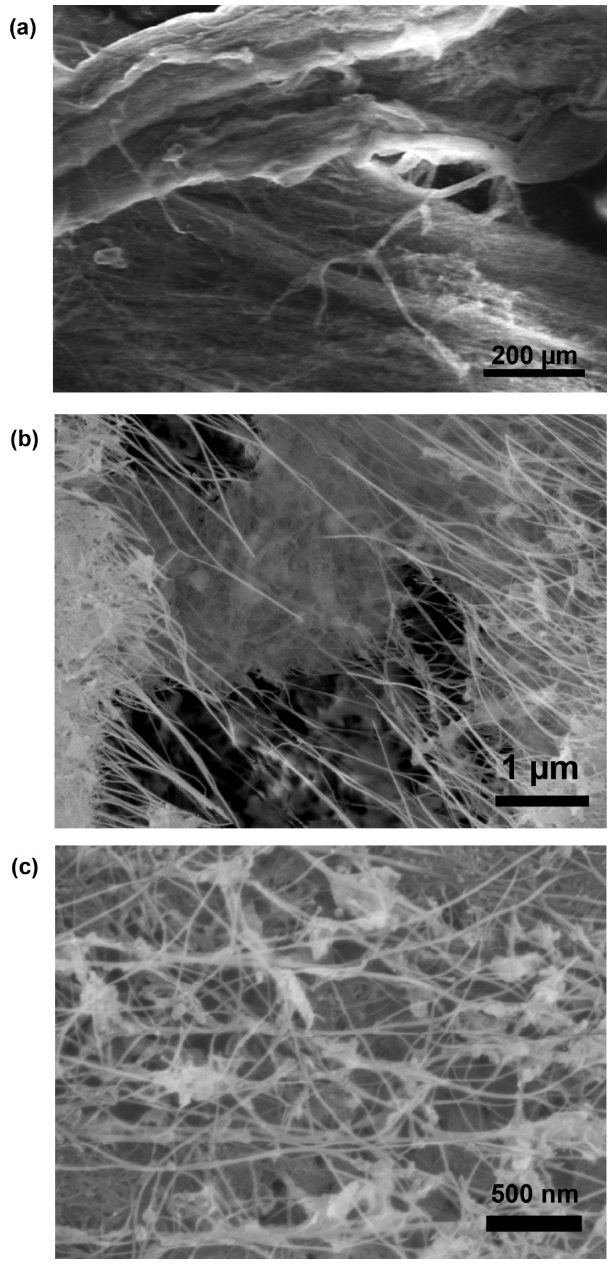

Figure 3. SEM images of as-synthesized BNNTs obtained from fibril-like material near center chamber. (a) Low magnification image of long fibrils. (b) Higher magnification image showing BNNT bundles. (c) Zoomed-in image of BNNT bundles and tubes. High-contrast spots are solidified unreacted boron droplets. To aid in high-resolution SEM imaging, a conventional thin gold film has been sputtered onto the specimens in b and c. Synthesis conditions: amorphous boron @ 150 mg/min; carrier gas N_2 @ 2.5 L/min; plasma gas N_2 @ 50 L/min; 40 kW plasma @ 45 psia.

The low-density spongy material consists of millimeter to centimeter (or longer) whispy fiber bundles, with rough macroscopic alignment of the fibrils (Figure 3a). At higher magnification (Figures 3b,c) the fibrils are seen to be composed of individual nanotubes (identified as pure BNNTs, see below); this and related imaging shows that the tubes have lengths exceeding tens of microns. At the zoomed-in scale (Figure 3c)

dx.doi.org/10.1021/nl5022915 | *Nano Lett.* 2014, 14, 4881−4886

the origin of the grayish patches of the bulk material is clearly revealed as unreacted nanoscale particles of solid boron (identified by EDAX) interspersed among the pure tubes and fibrils.

High-resolution TEM images of individual BNNTs within the fibrils are presented in Figure 4. Figure 4a shows a typical

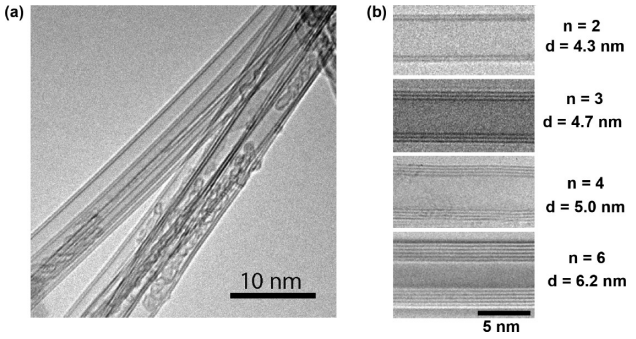

Figure 4. High-resolution TEM images of BNNTs produced by EPIC synthesis. (a) A bundle of double-wall BNNTs; (b) individual BNNTs with different number of walls indicated by *n* and outer tube diameter indicated by *d*. High crystallinity is apparent. Under these synthesis conditions 70% of the BNNTs are double wall, $n = 2$. Synthesis conditions: same as for Figure 3.

BNNT bundle, while Figure 4b shows details of individual tubes. Tubes with wall number, *n*, ranging from two to six are shown, with outer diameters spanning 4–6 nm. Our TEM analysis verifies the hollow, tubular nature of the BNNTs. Counting tubes in multiple TEM sessions shows that the majority of the BNNTs are double-walled (70%) with the next most predominant being triple walled (20%); this 90% distribution has diameters ranging from 2–6 nm. The majority of the remaining 10% of the BNNTs are multiwall nanotubes with wall number $n \geq 3$, with only a very sparing amount of $n = 1$ nanotubes (see below). The multiwall BNNTs are generally highly crystalline with straight walls with no "bamboo" or "Dixie-cup" like defects. The high crystallinity of the as-synthesized BNNTs is reconfirmed in selected area electron diffraction (data not shown). The structural quality of the tubes is significantly higher than that seen for most other BNNT synthesis techniques and is comparable to that for BNNTs produced by the laser vaporization method.[24]

Figure 5 shows an EELS spectrum from a BNNT collected from the fibril region. Prominent boron and nitrogen peaks with sp^2-hybridization signatures are clearly observed, yielding an atomic B/N ratio of 1.02, in agreement with unity expected for pure BNNTs. A small carbon peak arises from contamination from the carbon TEM support grid during measurement. Figure 6 shows a Raman spectrum for a BNNT, again collected from the fibril, chamber-center region. The peak at 1367 cm^{-1} is attributable to the E_{2g} vibration mode of sp^2-bonded BNNTs.[27] The fwhm is 11 cm^{-1}, which indicates highly crystalline "graphitic" BN.[28]

The preponderance of double-wall BNNTs in our EPIC synthesis method is consistent with the ionic nature of the B–N bond and the tendency for interplane B–N bonding (hence the stable A–A′ bonding structure of hBN). An interesting question concerns the stability of single-wall BNNTs (SWBNNTs). For carbon systems, single wall nanotubes are straightforward to synthesize en masse,[29] but for BN this has not been the case.[4,30] Within the (admittedly limited)

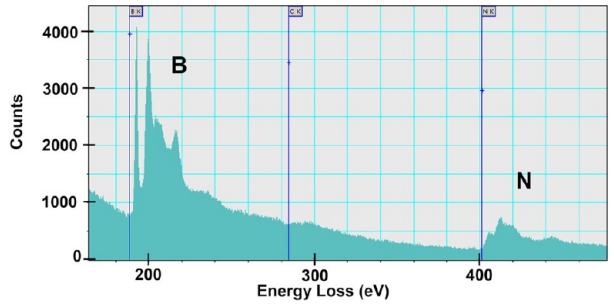

Figure 5. Electron energy loss spectroscopy (EELS) for BNNT produced by EPIC method. Boron and nitrogen peaks are clearly evident and indicate an atomic ratio B/N of 1:1, as expected for pure BN nanotubes. A very small carbon peak near 285 eV arises from contamination from the carbon support grid during measurement; the as-synthesized BNNTs contain no carbon. Synthesis conditions: same as for Figure 3.

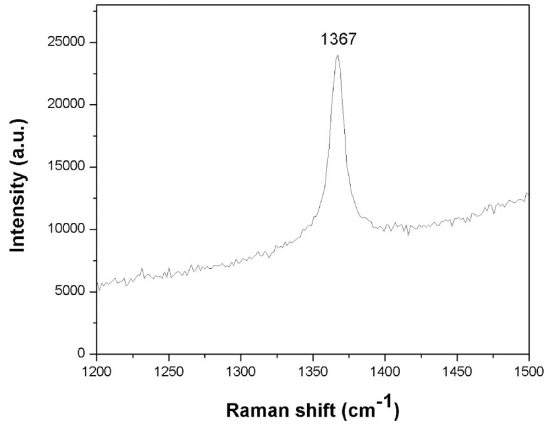

Figure 6. Raman spectrum of BNNT produced by EPIC. The peak position at 1367 cm^{-1} is characteristic of sp^2-bonded BN, and the sharpness of the peak is characteristic of highly crystalline BN. Synthesis conditions: same as for Figure 3.

parameter range we have explored for EPIC, we find some, but not many, SWBNNTs. Indeed, the SWBNNTs we do observe are not great in length, and at their ends they often morph into other lower symmetry, structurally tortured BN units.

The EPIC system displays great versatility for tuning synthesis conditions. Variable pressure, carrier gas, and feedstock type and injection rate all provide for a unique environment to grow not only high-quality, high-aspect-ratio BNNTs, but also other BN-based nanostructures. The experimental conditions under which various BN nanomaterials are synthesized can also elucidate the ways in which the nanostructures are formed. By tuning the reaction parameters, various forms of BN nanostructures can be targeted.

For BNNTs synthesis from pure boron and nitrogen, the overall reaction is

$$2B + N_2 \rightarrow 2BN \quad (1)$$

This reaction rate is expected to increase under high pressure of nitrogen, and indeed that is what is observed here. At 1 atm pressure, while some BNNTs are formed, there is also a considerable amount of boron that has not completely reacted with nitrogen to form BN. In this case there can be only a shell, or "nanococoon", of BN around the boron particles. Figure 7a shows examples of boron-filled BN nanococoons so produced.

dx.doi.org/10.1021/nl5022915 | *Nano Lett.* 2014, 14, 4881–4886

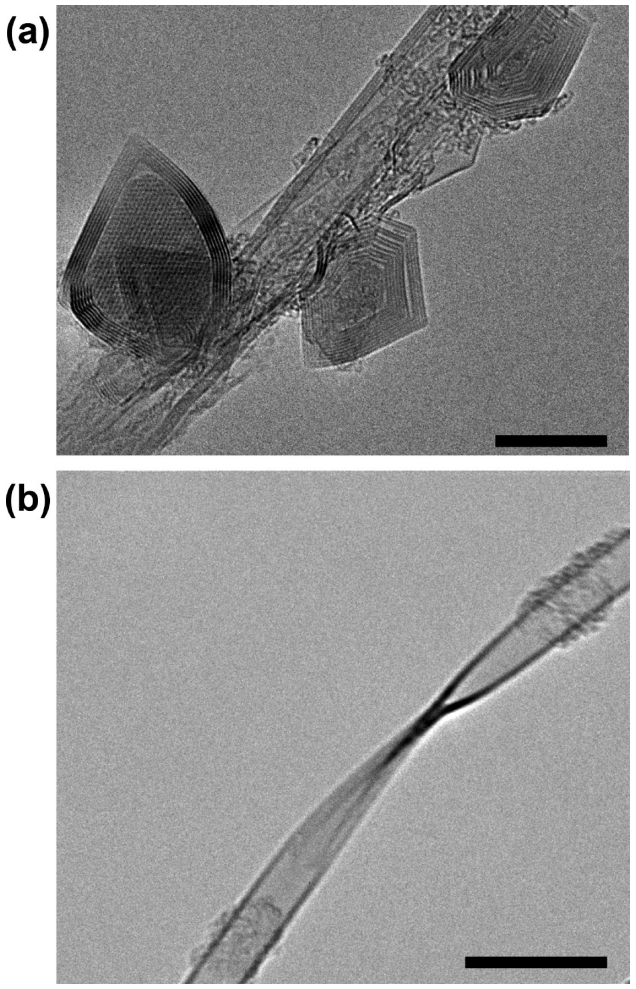

Figure 7. TEM images of (a) BN nanococoons, filled with boron, and (b) flattened, twisted BN nanoribbon derived from flattened BNNT. Under appropriate conditions (see text), the EPIC method directly produces a minority of such ribbons and cocoons, without any postprocessing requirement. Synthesis conditions: (a) amorphous boron @ 150 mg/min; carrier gas N_2 @ 2.5 L/min; plasma gas N_2 @ 50 L/min; 40 kW plasma @ 25 psia; (b) amorphous boron @150 mg/min; carrier gas N_2 @ 2.5 L/min; plasma gas N_2 @ 50 L/min; 40 kW plasma ramped from 15 to 45 psia.

At pressures above 2 atm, the concentration of these nanococoons begins to decrease, and at 3 atm and above, they compose only a very small fraction of the resulting product. While this indicates that, as previously proposed,[24] high-pressure nitrogen environments can assist high purity BNNT synthesis, it also hints at the mechanism of BNNT formation: as boron is injected into the plasma plume, it becomes a molten droplet. The surface of this droplet reacts with the nitrogen while within and as it exits the plasma plume. The higher pressure of nitrogen increases the energy density of the plasma plume and the collision rate of nitrogen atoms with the boron droplet and thereby shifts the reaction toward BN in eq 1. When the nitrogen pressure is relatively low, the boron does not react completely thus enabling BN nanococoons. As the nitrogen pressure increases, the boron droplet completely reacts forming mostly BNNTs. Hence, the EPIC system allows tailoring of BN-based nanoparticle growth, and thereby various forms of non-nanotube BN nanostructures can be produced in significant quantities (though in our preliminary studies not yet exclusively).

Along similar lines, under appropriate synthesis conditions the EPIC system can also form a large fraction of collapsed BNNTs. For carbon nanotubes, it has been shown that for some types of nanotubes (few enough wall number and large enough diameter), the more stable configuration for a nanotube is not the conventional "inflated" tube of circular cross-section, but rather a "collapsed" or flattened tube where the tube now resembles more a ribbon. Collapsed carbon nanotube ribbons have been experimentally observed.[31] Previous efforts have examined deformed BN nanostructures by high temperature metal-catalyzed reactions of BNNTs,[32] and alkali-driven "unzipping" of BNNTs has yielded BN-based ribbons,[33] but edge-free flattened-BN ribbons derived from unadulterated collapsed BNNTs have not been previously reported. These structures are of special interest as the flattening is predicted to dramatically alter the electronic structure of the tube,[34] allowing band gap engineering, and mechanically modulated optoelectronic devices.

Figure 7b shows a high-resolution TEM image of a collapsed BNNT, flattened into a twisted ribbon, produced by the EPIC method. To date, these structures have been only produced as minority phases in the synthesis of BNNTs, but it is possible that for some set of parameters within EPIC they can be the dominant (or only) synthesis product.

In summary, a versatile, scalable high-throughput synthesis method for the production of highly crystalline, low-wall-number, high aspect ratio BNNTs has been demonstrated. The direct-injection, extended pressure EPIC system allows for a wide range of synthesis parameters, including catalyst-free BNNT production at a rate thus far of 35 g/h, nearly 300 times the production rate of the laser vaporization method.[24] Additional BN-based nanostructures such as nanococoons and collapsed-tube nanoribbons are accessible. The EPIC method should find further application in other synthesis challenges, for example, alloy $B_xC_yN_z$ nanotubes,[34−36] and importantly other nanostructures containing elements in addition to or other than boron and nitrogen.

After the completion of this work, we became aware of a very recent online publication describing a related successful plasma synthesis method for BNNTs.[37] In the study of Kim et al., hBN powder is injected into a slightly reduced (i.e., slightly below atmospheric) pressure inductively coupled plasma, with an impressive BNNT production rate comparable to that reported here. Interestingly, the method of Kim et al. necessitates hydrogen gas, as well as preformed hBN precursor feedstock, for meaningful yield. In the extended-pressure EPIC method presented here, neither hydrogen nor hBN are necessary. Indeed, it appears that the "catalytic" activity of hydrogen in the Kim et al. method is obviated by a higher pressure nitrogen environment; similarly, the EPIC method is tolerant of a wider range of boron-containing feedstock (for example pure boron powder injection yields excellent results using higher-pressure plasma but is unsuccessful in the Kim et al. study).

AUTHOR INFORMATION

Corresponding Author

*E-mail: azettl@berkeley.edu.

Author Contributions

The experiments were conceived and designed by all authors. A.F. and T.P. carried out the synthesis runs. SEM imaging was carried out by A.F. and T.P. TEM imaging was performed by

dx.doi.org/10.1021/nl5022915 | *Nano Lett.* 2014, 14, 4881−4886

A.F., T.P., and W.M. EELS spectra were collected by A.F. and W.M. Raman spectra were taken by T.P. The manuscript was written by all authors.

Notes

The authors declare no competing financial interest.

■ ACKNOWLEDGMENTS

We thank C. Song for assistance with the EELS measurements. This research was supported in part by the Director, Office of Basic Energy Sciences, Materials Sciences and Engineering Division, of the U.S. Department of Energy under Contract DE-AC02-05CH11231, within the sp^2-bonded Materials Program, which provided for the design, construction, and execution of the experiment; the National Science Foundation under grant EEC-0832819, which provided for salary support (WM) and Raman characterization; and by the National Center for Electron Microscopy of the Lawrence Berkeley National Laboratory, under Contract DE-AC02-05CH11231, which provided for EELS characterization.

■ REFERENCES

(1) Chopra, N. G.; Luyken, R. J.; Cherrey, K.; Crespi, V. H.; Cohen, M. L.; Louie, S. G.; Zettl, A. *Science* **1995**, *269* (5226), 966−967.
(2) Rubio, A.; Corkill, J. L.; Cohen, M. L. *Phys. Rev. B* **1994**, *49* (7), 5081−5084.
(3) Iijima, S. *Nature* **1991**, *354* (6348), 56−58.
(4) Cohen, M. L.; Zettl, A. *Phys. Today* **2010**, *63* (11), 34−38.
(5) Blase, X.; Rubio, A.; Louie, S. G.; Cohen, M. L. *Europhys. Lett.* **1994**, *28* (5), 335−340.
(6) Ishigami, M.; Sau, J. D.; Aloni, S.; Cohen, M. L.; Zettl, A. *Phys. Rev. Lett.* **2005**, *94* (5), 056804.
(7) Jaffrennou, P.; Barjon, J.; Lauret, J. S.; Maguer, A.; Golberg, D.; Attal-Trétout, B.; Ducastelle, F.; Loiseau, A. *Phys. Status Solidi B* **2007**, *244* (11), 4147−4151.
(8) Chang, C. W.; Han, W. Q.; Zettl, A. *Appl. Phys. Lett.* **2005**, *86* (17), 173102.
(9) Mele, E. J.; Král, P. *Phys. Rev. Lett.* **2002**, *88* (5), 056803.
(10) Chen, X.; Wu, P.; Rousseas, M.; Okawa, D.; Gartner, Z.; Zettl, A.; Bertozzi, C. R. *J. Am. Chem. Soc.* **2009**, *131* (3), 890.
(11) Mickelson, W.; Aloni, S.; Han, W. Q.; Cumings, J.; Zettl, A. *Science* **2003**, *300* (5618), 467−469.
(12) Cumings, J.; Zettl, A. *Solid State Commun.* **2004**, *129* (10), 661−664.
(13) Hilder, T. A.; Gordon, D.; Chung, S. H. *Small* **2009**, *5* (19), 2183−2190.
(14) Zhi, C.; Bando, Y.; Tang, C.; Honda, S.; Kuwahara, H.; Golberg, D. *J. Mater. Res.* **2006**, *21* (11), 2794−2800.
(15) Lahiri, D.; Hadjikhani, A.; Zhang, C.; Xing, T.; Li, L. H.; Chen, Y.; Agarwal, A. *Mater. Sci. Eng.: A* **2013**, *574* (0), 149−156.
(16) Cumings, J.; Zettl, A. *Chem. Phys. Lett.* **2000**, *316* (3−4), 211−216.
(17) Golberg, D.; Bando, Y.; Eremets, M.; Takemura, K.; Kurashima, K.; Yusa, H. *Appl. Phys. Lett.* **1996**, *69* (14), 2045−2047.
(18) Lourie, O. R.; Jones, C. R.; Bartlett, B. M.; Gibbons, P. C.; Ruoff, R. S.; Buhro, W. E. *Chem. Mater.* **2000**, *12* (7), 1808−+.
(19) Zhi, C. Y.; Bando, Y.; Tan, C. C.; Golberg, D. *Solid State Commun.* **2005**, *135* (1−2), 67−70.
(20) Shimizu, Y.; Moriyoshi, Y.; Tanaka, H.; Komatsu, S. *Appl. Phys. Lett.* **1999**, *75* (7), 929−931.
(21) Chen, Y.; Chadderton, L. T.; FitzGerald, J.; Williams, J. S. *Appl. Phys. Lett.* **1999**, *74* (20), 2960−2962.
(22) Han, W. Q.; Bando, Y.; Kurashima, K.; Sato, T. *Appl. Phys. Lett.* **1998**, *73* (21), 3085−3087.
(23) Han, W. Q.; Mickelson, W.; Cumings, J.; Zettl, A. *Appl. Phys. Lett.* **2002**, *81* (6), 1110−1112.
(24) Smith, M. W.; Jordan, K. C.; Park, C.; Kim, J. W.; Lillehei, P. T.; Crooks, R.; Harrison, J. S. *Nanotechnology* **2009**, *20* (50), 505604.
(25) Keun, K. S.; German, C.-S.; Christopher, T. K.; Matej, I.; Benoit, S.; Gervais, S. *J. Phys. D: Appl. Phys.* **2007**, *40* (8), 2375.
(26) Zettl, A. K. Method and Device to Synthesize Boron Nitride Nanotubes and Related Nanoparticles. Patent App. No. US2013064750, Mar 21, 2011.
(27) Wu, J.; Han, W.-Q.; Walukiewicz, W.; Ager, J. W.; Shan, W.; Haller, E. E.; Zettl, A. *Nano Lett.* **2004**, *4* (4), 647−650.
(28) Nemanich, R. J.; Solin, S. A.; Martin, R. M. *Phys. Rev. B* **1981**, *23* (12), 6348−6356.
(29) Terrones, M. *Annu. Rev. Mater. Res.* **2003**, *33*, 419−501.
(30) Loiseau, A.; Willaime, F.; Demoncy, N.; Hug, G.; Pascard, H. *Phys. Rev. Lett.* **1996**, *76* (25), 4737−4740.
(31) Chopra, N. G.; Zettl, A. *Solid State Commun.* **1998**, *105* (5), 297−300.
(32) Tang, C.; Bando, Y.; Ding, X.; Qi, S.; Golberg, D. *J. Am. Chem. Soc.* **2002**, *124* (49), 14550−14551.
(33) Erickson, K. J.; Gibb, A. L.; Sinitskii, A.; Rousseas, M.; Alem, N.; Tour, J. M.; Zettl, A. K. *Nano Lett.* **2011**, *11* (8), 3221−3226.
(34) Kim, Y. H.; Chang, K. J.; Louie, S. G. *Phys. Rev. B* **2001**, *63* (20), 205408.
(35) Miyamoto, Y.; Rubio, A.; Cohen, M. L.; Louie, S. G. *Phys. Rev. B* **1994**, *50* (7), 4976−4979.
(36) Weng-Sieh, Z.; Cherrey, K.; Chopra, N. G.; Blase, X.; Miyamoto, Y.; Rubio, A.; Cohen, M. L.; Louie, S. G.; Zettl, A.; Gronsky, R. *Phys. Rev. B* **1995**, *51* (16), 11229−11232.
(37) Kim, K. S.; Kingston, C. T.; Hrdina, A.; Jakubinek, M. B.; Guan, J.; Plunkett, M.; Simard, B. *ACS Nano* **2014**, *8*, 6211−6220.